Modeling Strain-Rate Dependent Behavior of KR_0-Consolidated Soft Clays

Li-Zhong Wang[1]; Han-Bo Dan, Ph.D.[2]; and Ling-Ling Li, Ph.D.[3]

Abstract: An anisotropic elastic-viscoplastic constitutive model is developed for K_0-consolidated soft clays in general stress space. Two surfaces are assumed to exist for any loading stress as the loading surface and the reference surface. The scalar multiplier is established by the viscoplastic volumetric strain rate under a one-dimensional straining condition. This model can adequately simulate the stress–strain behavior of undrained triaxial constant strain rate shear tests and undrained creep tests for K_0-consolidated clays. The strain-rate dependencies of preconsolidation pressure and undrained shear strength are investigated in analytical formulations, and the similarities and differences of their corresponding strain-rate parameters are examined. **DOI: 10.1061/(ASCE)EM.1943-7889.0000371.** *© 2012 American Society of Civil Engineers.*

CE Database subject headings: Clays; Viscoplasticity; Anisotropy; Strain rates; Shear strength.

Author keywords: Soft clays; Elastic viscoplasticity; Anisotropy; Strain-rate dependency; Preconsolidation pressure; Undrained shear strength.

Introduction

The viscous behavior of soft soils is evident in creep and the types of strain-rate dependent phenomena, which have been studied by many researchers since the early 1920s (Graham et al. 1983; Leroueil et al. 1985; Sheahan et al. 1996; Zhu and Yin 2000; Cheng and Yin 2005). From the 1960s to the 1990s, many laboratory studies were conducted in odometer tests, and mathematical formulations of the one-dimensional (1D) phenomena were proposed (Bjerrum 1967; Leroueil et al. 1985; Yin and Graham 1994). The pioneering work provides a fundamental tool for further understanding the viscous behavior of soils and developing rate-dependent constitutive models in general stress states.

Some general three-dimensional (3D) creep models were directly extended from the 1D differential formulations, such as those suggested by Yin and Graham (1999); Vermeer and Neher (2000); Zhou et al. (2005); Leoni et al. (2008); and Kelln et al. (2008). Most of these models adopted yield ellipses (inclined or not) and assumed these ellipses to be contours of viscoplastic volumetric strain rates. Although this assumption is convenient, it is arguable. In the framework of critical state soil mechanics (Wood 1990), the size of the yield locus is assumed to change only when plastic changes of soil volume occur. If the loading path is just along the yield locus, it will not cause any plastic changes of volume. Therefore, the yield locus can be considered to be the contour of plastic volumetric strain. However, the plastic strain rates vectors are normal to the yield locus based on the associated flow rule. As shown Fig. 1(a), for special Point C where the soil is at the critical stress state and tends to fail, the plastic volumetric rate equals to zero. Whereas at other points on the same yield locus (e.g., Point A of isotropic stress state or Point B of AD straining), the plastic volumetric rates are not zero with their directions parallel to the p' axis. It demonstrates that the yield locus is not the contour of plastic volumetric strain rate. The same conclusion can also be drawn when the effect of anisotropy is taken into account, as shown in Fig. 1(b), where the yield surfaces are inclined ellipses. Therefore, in the process of formulating the general 3D creep constitutive model, it is unreasonable to assume that the viscoplastic volumetric strain rate is constant on the same loading or flow surface.

The overstress theory, proposed by Perzyna (1963), is a classical concept in the study of viscous solid behavior, and considerable success has been achieved in modeling the time effects of soft soils by using this concept (Adachi and Oka 1982; Desai and Zhang 1987; Kutter and Sathialingam 1992; Hinchberger and Rowe 2005). Models based on this framework agree commonly with the assumption that only the changes of effective stresses outside the current static yield surface f_s lead to the onset of time-dependent viscoplastic deformations, and the viscoplastic scalar multiplier $\varphi(F)$ is introduced to calculate the viscoplastic strain rates. $\varphi(F)$ depends on the difference between the current stress state and the static field surface f_s, which can be expressed by the so-called "excess stress function" F. Thus, $\varphi(F)$ must be constant for any stress state on the same loading surface, and its functional form can be experimentally or theoretically determined, although this has not been widely presented so far. In addition, because the static yield surface f_s is an elastic nucleus, the original overstress type models lack the capability in modeling the tertiary creep and the time-dependent behavior of heavily overconsolidated soils (Liingaard et al. 2004). Therefore, some models do not define an elastic nucleus, and a mapping rule is adopted to model the viscoplastic strains for all states of stresses (Kutter and Sathialingam 1992).

[1]Professor, College of Civil Engineering and Architecture, Zhejiang Univ., Hangzhou 310058, Zhejiang, China. E-mail: wlzzju@163.com

[2]Designer, Zhejiang Electric Power Design Institute, Hangzhou 310012, Zhejiang, China; formerly, College of Civil Engineering and Architecture, Zhejiang Univ., Hangzhou 310058, Zhejiang, China. E-mail: dan_zju@163.com

[3]College of Civil Engineering and Architecture, Zhejiang Univ., Hangzhou 310058, Zhejiang, China (corresponding author). E-mail: lingzju@126.com
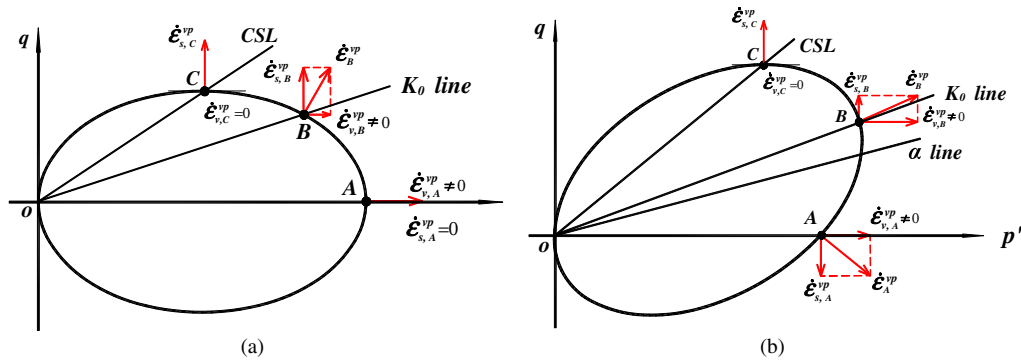
Fig. 1. The viscoplatic strain rates of soils under different stress states; (a) isotropically consolidated clays; (b) K_0-consolidated clays

Most of the studies were carried out on the basis of isotropically consolidated reconstituted soils tests. However, the soils are mostly in a K_0-consolidation condition with zero lateral deformation in their sedimentary process. This initial stress-induced anisotropy is an important factor that must be considered both in laboratory tests and constitutive modeling. Wang et al. (2008) derived the theoretical formulas for predicting the undrained shear strength of K_0-consolidated soft soils. Cheng and Yin (2005) performed laboratory tests to study the strain-rate dependent behavior of K_0-consolidated Hong Kong natural marine clays. Zhou et al. (2005) and Leoni et al. (2008) presented their respective anisotropic elastic-viscoplastic (EVP) models with the assumption that the loading surfaces are contours of the viscoplastic volumetric strain rates. Nevertheless, it was found that the laboratory and constitutive modeling studies on the rate-dependent behavior of K_0-consolidated clays remain limited.

In this paper, a new general 3D anisotropic EVP model is presented to simulate the strain-rate dependent behavior of K_0-consolidated clays. The constitutive equations are derived on the basis of the overstress concept, assuming inclined ellipses as contours of the viscoplastic scalar multiplier φ. The reference surface corresponding to the normally consolidated state is defined to substitute for the static yield surface f_s, and a radial mapping rule is used in the proposed model. It is shown that various types of stress–strain–time behavior are modeled adequately, including strain-rate effects in undrained shear tests and the accelerated creep. The strain-rate dependencies of the preconsolidation pressures and undrained shear strengths are investigated and their differences are examined. The model can be extended to consider the rotational hardening for plastic anisotropic evolution.

Mathematical Formulations of Three-Dimensional Elastic-Viscoplastic Model

Fundamental Assumptions and Basic Equations

The stress invariants mean effective stress p' and deviator stress q are defined as

$$p' = \sigma'_{kk}/3 = (\sigma'_{11} + \sigma'_{22} + \sigma'_{33})/3 \quad \text{and} \quad q = \sqrt{3 s_{ij} s_{ij}/2} \tag{1}$$

where the subindexes $i = 1, 2, 3$ and $j = 1, 2, 3$, σ'_{ij} = the effective stress vector, s_{ij} = the deviator stress tensor $s_{ij} = \sigma'_{ij} - p' \delta_{ij}$, and δ_{ij} = the Kronecker delta, $\delta_{ij} = 1$ if $i = j$, and $\delta_{ij} = 0$ if $i \neq j$.

Like most of the time-dependent constitutive models, an assumption is adopted that if there is no "instant" plastic strains

and all inelastic strains are viscoplastic, the total strain rate $\dot{\varepsilon}_{ij}$ is expressed as

$$\dot{\varepsilon}_{ij} = \dot{\varepsilon}^e_{ij} + \dot{\varepsilon}^{vp}_{ij} \tag{2}$$

where $\dot{\varepsilon}^e_{ij}$ and $\dot{\varepsilon}^{vp}_{ij}$ are the elastic and viscoplastic strain rate tensors, respectively, and the overdot denotes the rate of a variable.

The elastic strains are assumed to be time-independent, and $\dot{\varepsilon}^e_{ij}$ can be obtained as

$$\dot{\varepsilon}^e_{ij} = \frac{\kappa}{3V_i} \frac{\dot{p}'}{p'} \delta_{ij} + \frac{1}{2G} \dot{s}_{ij} \tag{3}$$

where κ = the recompression index in natural log scale, $V_i = 1 + e_i$ is the initial specific volume, and e_i is the initial void ratio before loading. The shear modulus G is related to the bulk modulus K and Poisson's ratio ν, $G = 3(1 - 2\nu)K/[2(1 + \nu)]$, where $K = V_i p'/\kappa$.

The rate equation for $\dot{\varepsilon}^{vp}_{ij}$ is based on a generalization of the overstress theory of Perzyna (1963), and a similar viscoplastic scalar multiplier φ, which is defined in the following section, is used in the present formulations. It is assumed that two surfaces exist for any loading history, as shown in Fig. 2, as follows:

1. Loading surface ($f = 0$): a rate sensitive surface of constant φ, containing the current stress state of the soil element. This is analogous to the dynamic surface ($f_d = 0$) in Perzyna (1963).
2. Reference surface ($\bar{f} = 0$): a work-hardening surface of constant φ on which soil has been consolidated for a reference time t_0. The normal consolidation line (NCL) is commonly obtained from the standard 24-h oedometer test with stepwise loading (MSL$_{24h}$), and so the corresponding value of t_0 is taken as 24 h. Different from the static yield surface f_s of Perzyna (1963), the reference surface is not an elastic nucleus,
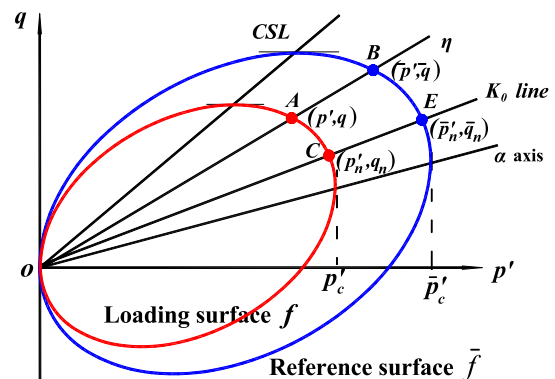

Fig. 2. Schematic figure of the loading and reference surfaces

but corresponds to stress states of normal consolidation. The current stress state on the loading surface is allowed to be inside, outside, or on the reference surface. When loads are applied to soil, the sizes of loading surface and reference surface change simultaneously, whose differences depend on the current viscoplastic strain rate of soil.

A radial mapping rule with the projection center at the origin of stress space is used in the present formulation. The mapping rule is defined to map the current stress state σ'_{ij} to its corresponding reference state, as shown in Fig. 2. As shown in the following, taking a radial mapping rule can be adequate for 1D and triaxial loadings that are typical cases of loading histories, although there may be some overprediction of undrained shear stress for dilative soil (e.g., heavily overconsolidated clay). However, for strongly nonproportional loading paths (e.g., loadings with stress reversal or cyclic loadings), some deficiencies may occur. One solution of this problem can be generalization of the mapping rule to allow for a projection center away from the origin, and kinematic hardening and evolution of the relocatable projection center are further adopted (Kutter and Sathialingam 1992; Li and Dafalias 2004). However, this kind of solution will make the presented model much more complicated. This work employs radial mapping for simplicity.

To consider the initial stress-induced anisotropy of natural clays, the loading and reference surfaces are supposed to be inclined ellipses, as shown in Fig. 2. Experimental evidence from Graham et al. (1983) suggest that an associated flow rule is a reasonable assumption for natural clays when combined with an inclined yield surface.

In this EVP model, an associated flow rule is adopted, and $\dot{\varepsilon}^{vp}_{ij}$ is given as

$$\dot{\varepsilon}^{vp}_{ij} = \phi \frac{\partial f}{\partial \sigma'_{ij}} \tag{4}$$

where the viscoplastic scalar multiplier ϕ represents the difference between the current stress σ'_{ij} and the reference stress $\bar{\sigma}'_{ij}$. The scalar multiplier ϕ in this work is defined for all values of f and $\bar{f}$, while the $\phi(F)$ in the original overstress theory is defined only for cases that $f_d > f_s$.

Functional Form of Loading Surface and Reference Surface

As shown in Fig. 2, the loading surfaces f and reference surfaces $\bar{f}$ are inclined ellipses in the $p' - q$ plane for K_0-consolidated clays,

and their expressions are the same as those suggested by Wheeler and Näätänen (2003)

$$f = \frac{(M^2 - \alpha^2) + (q/p' - \alpha)^2}{M^2 - \alpha^2} p' - p'_c = 0 \tag{5}$$

$$\bar{f} = \frac{(M^2 - \alpha^2) + (\bar{q}/\bar{p}' - \alpha)^2}{M^2 - \alpha^2} \bar{p}' - \bar{p}'_c = 0 \tag{6}$$

where η = the effective stress ratio defined as $\eta = q/p' = \bar{q}/\bar{p}'$ according to radial mapping rule, and M = the critical state value of η p'_c and $\bar{p}'_c$ are the mean effective stresses, where the loading surface and reference surface intercept the α line, respectively.

The α line defines the inclination of the elliptical loading and reference surfaces, which represents the effects of plastic anisotropy. In this paper, the effects of the initial stress-induced anisotropy are considered, and the evolution of anisotropy during the soil deformation process is ignored for simplicity, so α remains constant as its initial value α_0. Actually, this EVP framework can be extended to consider the rotational hardening for plastic anisotropic evolution. According to Wheeler and Näätänen (2003), the value of α_0 can be obtained from the 1D straining compression

$$\alpha_0 = (\eta^2_{K_{0nc}} + 3\eta_{K_{0nc}} - M^2)/3 \tag{7}$$

where for normally K_0-consolidated soils, the initial effective stress $\eta_{K_{0nc}} = 3(1 - K_{0nc})/(1 + 2K_{0nc})$, and K_{0nc} can be calculated by $K_{0nc} = 1 - \sin \phi'$. If the soil is isotropically consolidated, $\alpha_0 = 0$; consequently, the loading surfaces and reference surfaces become symmetrical to the isotropic axis.

Derivation of the Viscoplastic Scalar Multiplier ϕ

Both the loading surface f and the reference surface $\bar{f}$ are contours of viscoplastic scalar multiplier ϕ. Therefore, the value of ϕ for a general stress state (e.g., Point A in Fig. 2) is equal to that for other stress states on the same loading surface (e.g., Point C in the 1D straining condition in Fig. 2), whose functional expression can be established from the volumetric creep strain rate in the 1D straining.

To appropriately express the viscoplastic strain rate in the 1D straining, absolute time t is adopted in this paper. Standard oedometer tests are most often carried out with 24-h load steps, and samples are compressed until the NCL is reached [blocked in Fig. 3(a)]. Thus, the absolute time of an arbitrary state on the NCL is just equal to the real loading duration (i.e., $t_0 = 24$ h). The NCL is taken as
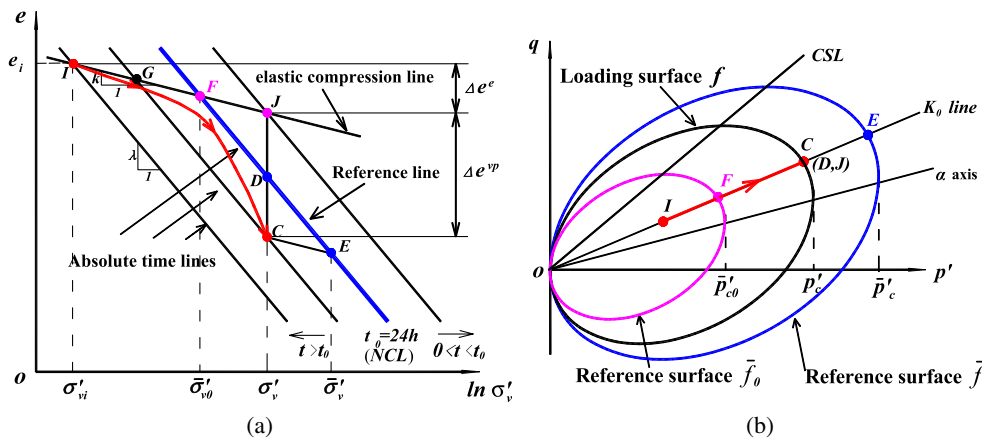

Fig. 3. Relative locations of stress states and reference states during one-dimensional compression (a) in the compression plane and the (b) in the $p' - q$ plane

the reference line for other state points in the 1D compression plane.

In the 1D straining condition shown in Fig. 3(a), it can be assumed that the current state Point C (σ'_v, e) is reached by an arbitrary compression path from an initial state Point I (σ'_{vi}, e_i), with the load imposed on the soil element increasing from σ'_{vi} to σ'_v. No matter what the $e - \ln \sigma'_v$ path is, the reference state of Point C must be unique, which is the quasi-preconsolidation stress Point E on the NCL. In addition, the normally consolidated state under the same vertical effective stress σ'_v can be also found as Point D. Then, a geometric relationship between Point C, Point D, and Point E in Fig. 3(a) exists as follows:

$$\Delta e_{DC} + \Delta e_{CE} = \Delta e_{DE} \tag{8}$$

where Δe_{DC} = the change of void ratio due to creep from Point D to C under constant stress, and Δe_{CE} and Δe_{DE} are, respectively, the elastic and total compressions as the stress increases from σ'_v to $\bar{\sigma}'_v$ in the MSL$_{24h}$ test. With some well-known formulations in the traditional soil mechanics, Eq. (8) changes to

$$\psi \ln \frac{t}{t_0} + \kappa \ln \frac{\bar{\sigma}'_v}{\sigma'_v} = \lambda \ln \frac{\bar{\sigma}'_v}{\sigma'_v} \tag{9}$$

where $\kappa = C_r / \ln 10$, $\lambda = C_c / \ln 10$, C_r and C_c = the recompression and compression index of natural clays, respectively; $\psi = C_{\alpha e} / \ln 10$, and $C_{\alpha e}$ = the coefficient of secondary compression.

From Eq. (9), the absolute time of point C is obtained as

$$t = t_0 \cdot (\bar{\sigma}'_v / \sigma'_v)^{(\lambda - \kappa)/\psi} \tag{10}$$

During the loading process from Point I to Point C, the total change of soil volume is quantitatively equal to the sum of the total elastic part Δe_{IJ} and the total viscoplastic part Δe_{JC}, as shown in Fig. 3(a). Point J is just an auxiliary point on the elastic compression line with the same vertical stress as Point C, and its reference state is Point F on the NCL, which corresponds to the initial yield state obtained from the standard MSL$_{24h}$ tests. Because the geometric relationship $\Delta e_{JC} = \Delta e_{JD} + \Delta e_{DC} = \Delta e_{FD} - \Delta e_{FJ} + \Delta e_{DC}$ exists, the total time-dependent irrecoverable strains during this process can be calculated as

$$\varepsilon_{vn}^{vp} = \frac{\lambda - \kappa}{V_i} \ln \left(\frac{\sigma'_v}{\bar{\sigma}'_{v0}} \right) + \frac{\psi}{V_i} \ln \left(\frac{t}{t_0} \right) \tag{11}$$

where the subscript $n = 1D$ straining condition, and $\bar{\sigma}'_{v0}$ = the preconsolidation stress corresponding to the initial yield Point F measured from the standard MSL$_{24h}$ tests with $\bar{\sigma}'_{v0} = \bar{\sigma}'_{v0} = \sigma'_{p,24h}$.

By incorporating Eq. (11) and Eq. (10), the viscoplastic volumetric strain rate of the current Point C is

$$\dot{\varepsilon}_{vn}^{vp} = \frac{\psi}{V_i} \cdot \frac{1}{t} = \frac{\psi}{V_i t_0} \left(\frac{\sigma'_v}{\bar{\sigma}'_v} \right)^{(\lambda-\kappa)/\psi} \tag{12}$$

It demonstrates that the creep strain rate $\dot{\varepsilon}_{vn}^{vp}$ is dependent on the difference between the current stress and its reference stress, but independent of the $e - \ln \sigma'_v$ path. Therefore, the compression lines parallel to the NCL are lines of constant absolute time or creep strain rate. During a creep process, the corresponding reference stress $\bar{\sigma}'_v$ increases with the absolute time t, then the calculated creep strain rate from Eq. (12) tends to negligible, so the concept of "limited time line" suggested by Yin and Graham (1994) is not used for simplification in this model.

The corresponding relationships in the stress space are shown as Fig. 3(b). In the $p' - q$ plane, Point C and Point D coincide with

each other because of their same stress state, but their corresponding reference states are quite different due to their different strain rates. For Point C, which is at the so-called overconsolidated state, the reference surface is outside the loading surface, and the creep rate is very low. Point D corresponds to a special condition that the soil is normally consolidated, and the reference surface coincides with the loading surface. In addition, it is important to realize that Eq. (10) and Eq. (12) are also suitable for states located above the NCL, where the current stresses become larger than their reference stresses and the creep rates are very high.

On the NCL, the reference stress increases during creep and satisfies the following relationship

$$\bar{\sigma}'_v = \bar{\sigma}'_{v0} \cdot \exp(\varepsilon_v^{vp} / [(\lambda - \kappa)/V_i]) \tag{13}$$

$$\dot{\bar{\sigma}}'_v / \bar{\sigma}'_v = \dot{\varepsilon}_{vn}^{vp} / [(\lambda - \kappa)/V_i] \tag{14}$$

Incorporating Eq. (12) with Eq. (4), the functional form of ϕ in the 1D straining condition can be derived

$$\phi = \frac{\dot{\varepsilon}_{vn}^{vp}}{(\partial f/\partial p')_n} = \frac{\psi}{V_i t_0} \left(\frac{\sigma'_v}{\bar{\sigma}'_v} \right)^{\frac{\lambda-\kappa}{\psi}} \cdot \frac{M^2 - \alpha_0^2}{M^2 - \eta_{K_{0nc}}^2} \tag{15}$$

where $\bar{\sigma}'_v$ is expressed as in Eq. (13).

The expression of ϕ for a general stress state can be directly obtained from the relationship $\phi = \phi_n$. Because of the radial mapping rule and the similarity of loading and reference surfaces, $\sigma'_v / \bar{\sigma}'_v = p'_c / \bar{p}'_c$, and the expression of ϕ becomes

$$\phi = \frac{\psi}{V_i T_0} \left(\frac{p'_c}{\bar{p}'_c} \right)^{\frac{\lambda-\kappa}{\psi}} \cdot \frac{M^2 - \alpha_0^2}{M^2 - \eta_{K_{0nc}}^2} \tag{16}$$

with

$$\bar{p}'_c = \bar{p}'_{c0} \cdot \exp(\varepsilon_v^{vp} / [(\lambda - \kappa)/V_i]) \tag{17}$$

where $\bar{p}'_{c0}$ corresponds to the reference surface passing through the initial yield state from the standard MSL$_{24h}$ tests, that is, the reference surface $\bar{f}_0$ in Fig. 3(b) which is analogous to the initial yield surface in the traditional plasticity.

The description of the general 3D model is now complete, and it can be summarized as

$$\dot{\varepsilon}_{ij} = \frac{\kappa}{3V_i} \frac{\dot{p}'}{p'} \delta_{ij} + \frac{1}{2G} \dot{s}_{ij} + \frac{\psi}{V_i t_0} \left(\frac{p'_c}{\bar{p}'_c} \right)^{\frac{\lambda-\kappa}{\psi}} \cdot \frac{M^2 - \alpha_0^2}{M^2 - \eta_{K_{0nc}}^2} \cdot \frac{\partial f}{\partial \sigma'_{ij}} \tag{18}$$

Note that the viscoplastic scalar multiplier ϕ is positive, whereas the negative viscoplastic strain rates are generated by the partial derivatives of the loading function $\partial f/\partial \sigma'_{ij}$. Eq. (18) reveals that without a stress change, irrecoverable strains will continue to develop because of the time increment.

Determination of Parameters

The above 3D general constitutive equations involve six parameters as λ, κ, M, ν, αR_0, and ψ. λ and κ can be obtained from standard MSL$_{24h}$ loading and unloading tests, and M can be calculated by $M = 6 \sin \varphi'_c / (3 - \sin \varphi'_c)$ where φ'_c is the effective friction angle from triaxial compression tests. Poisson's ratio ν is usually 0.3 for soft clays. The expression of α_0 is given as Eq. (7), which can be considered as a function of φ'_c.

The viscous parameter ψ has the relationship of $\psi = C_\alpha / \ln 10$, and C_α is the traditional coefficient of secondary compression that can be measured from 1D oedometer creep tests. In this model, ψ is assumed to be constant in the whole creep process. Mesri and Castro (1987) showed that C_α relates to the compression index C_c, and C_α / C_c is almost constant for a given soil type. They also

indicated that $C_\alpha/C_c = 0.04 \pm 0.01$ for inorganic clays and silts, but 0.05 ± 0.01 for organic clays and silts. Now that there is no exact measured value of ψ, these empirical relationships can be used in simulation.

Rate-Dependent Effects of Preconsolidation Pressure and Undrained Shear Strength

The preconsolidation pressure and undrained shear strength are two basic parameters for the design of geotechnical structures. Many test results demonstrate that these two factors are strain-rate dependent and that they may increase by around 10% for a tenfold increase in strain rates. Based on the present EVP constitutive model, the rate-dependent effects of these two factors are theoretically formulated as follows.

Strain-Rate Effects on Preconsolidation Pressure

In the 1D straining, the vertical strain of soil element ε_z is equal to its volumetric strain ε_{vn}. From a series of tests (e.g., constant rate of strain [CRS] tests, step-changed strain rate tests, multistepped loading tests, long-term creep tests), Leroueil et al (1985) showed that the $(\sigma_v', \varepsilon_z, \dot{\varepsilon}_z)$ relationship could be simply described by two curves, one giving the variation of the preconsolidation pressure with strain rate $[\sigma_p' = f(\dot{\varepsilon}_z)]$ and the other presenting the normalized stress–strain curve $[\sigma_v'/\sigma_p' = g(\varepsilon_z)]$. The rate dependency of preconsolidation pressure directly reflects the strain-rate effect on the soil's 1D compression behavior. In this EVP formulation, it can be assumed that the total strain rate $\dot{\varepsilon}_z$ is equal to its viscoplastic part $\dot{\varepsilon}_z^{vp}$ (i.e., $\dot{\varepsilon}_z \approx \dot{\varepsilon}_z^{vp}$) after the soil yields. Therefore, the present constant absolute time lines also correspond to lines of constant strain rate, which can fairly simulate the strain-rate dependency of the compression behavior of soil in 1D straining.

With different strain rates $\dot{\varepsilon}_z$, the soil starts to yield at different states that can be expressed as crossing points of the elastic compression line and different absolute time lines (e.g., Point G, Point F, or Point J in Fig. 3(a)), and the apparent preconsolidation pressures σ_p' have different values accordingly. As the aforementioned definition, all these initial yield points have a unique reference state, which is Point F on the NCL. Based on Eq. (12), the relationship between $\dot{\varepsilon}_z$ and σ_p' goes to

$$\dot{\varepsilon}_z \approx \dot{\varepsilon}_z^{vp} = \cdot \frac{\psi}{V_i t_0} \left(\frac{\sigma_p'}{\sigma_{p,24h}'}\right)^{(\lambda-\kappa)/\psi} \quad (19)$$

Then, the apparent preconsolidation pressure σ_p' can be obtained

$$\sigma_p' = (\dot{\varepsilon}_z/\dot{\varepsilon}_{z,24h})^{(\psi/\lambda)/\Lambda} \cdot \sigma_{p,24h}' \quad (20)$$

where $\Lambda = 1 - \kappa/\lambda$ = the compression parameter; $\sigma_{p,24h}'$ = the preconsolidation pressure measured from the standard MSL_{24h} test, and $\dot{\varepsilon}_{z,24h} = \dot{\varepsilon}_{z,24h} = \varepsilon_{z,24h} \approx \dot{\varepsilon}_{z,24h}^{vp} = \psi/(V_i t_0)$.

Corresponding to different strain rates $\dot{\varepsilon}_{z1}$ and $\dot{\varepsilon}_{z2}$, the different apparent preconsolidation pressures σ_{p1}' and σ_{p2}' have the following relationship

$$\sigma_{p2}'/\sigma_{p1}' = (\dot{\varepsilon}_{z2}/\dot{\varepsilon}_{z1})^{(\psi/\lambda)/\Lambda} \quad (21)$$

Referring to Graham et al. (1983), a strain-rate parameter ρ_n can be defined to express the strain-rate dependency of the apparent preconsolidation pressure

$$\rho_n = (\Delta\sigma_p'/\sigma_{p1}')/\Delta \log \dot{\varepsilon}_z \quad (22)$$

where $\Delta\sigma_p'$ = the increment of σ_p' as the strain rate increases from $\dot{\varepsilon}_{a1}$ to $\dot{\varepsilon}_{a2}$. If a tenfold increase occurs in strain rates ($\dot{\varepsilon}_{z2} = 10\dot{\varepsilon}_{z1}$), ρ_n is a constant

$$\rho_n = 10^{(\psi/\lambda)/\Lambda} - 1 = 10^{(C_\alpha/C_c)/\Lambda} - 1 \quad (23)$$

Strain-Rate Effects on Undrained Shear Strength

When the soil element is under triaxial shearing, its stresses and strains can be expressed as

$$p' = (\sigma_a' + 2\sigma_r')/3, \qquad q = \sigma_a' - \sigma_r', \qquad \dot{\varepsilon}_v = \dot{\varepsilon}_a + 2\dot{\varepsilon}_r,$$
$$\dot{\varepsilon}_s = 2/3(\dot{\varepsilon}_a - \dot{\varepsilon}_r) \quad (24)$$

where the subscripts a and r = the axial and radial directions, respectively.

From Eq. (18), the volumetric and deviatoric strain rates are given as follows:

$$\dot{\varepsilon}_v = \frac{\kappa}{3V_i} \cdot \frac{\dot{p}'}{p'} + \frac{\psi}{V_i t_0} \cdot \left(\frac{p_c'}{\bar{p}_{c0}'}\right)^{\frac{\lambda-\kappa}{\psi}} \cdot \exp\left(\frac{-\varepsilon_v^{vp}}{\psi/V_i}\right) \cdot \frac{M^2 - \eta^2}{M^2 - \eta_{K_{0nc}}^2} \quad (25a)$$

$$\dot{\varepsilon}_s = \frac{1}{3G} \cdot \dot{q} + \frac{\psi}{V_i t_0} \cdot \left(\frac{p_c'}{\bar{p}_{c0}'}\right)^{\frac{\lambda-\kappa}{\psi}} \cdot \exp\left(\frac{-\varepsilon_v^{vp}}{\psi/V_i}\right) \cdot \frac{2(\eta - \alpha_0)}{M^2 - \eta_{K_{0nc}}^2} \quad (25b)$$

If the soil elements are forbidden to drain during testing, their volumes must remain constant, then

$$\varepsilon_v^e + \varepsilon_v^{vp} = 0 \Rightarrow \varepsilon_v^{vp} = -\kappa/V_i \cdot \ln(p'/p_i') \quad (26)$$

where p_i' = the initial mean effective stress of soil before undrained shearing, $p_i' = (1 + 2K_0)/3\sigma_{vi}'$.

Under the undrained condition, the viscoplastic deviator strain rate $\dot{\varepsilon}_s^{vp}$ can be given as

$$\dot{\varepsilon}_s^{vp} = \frac{\psi}{V_i t_0} \cdot \left(\frac{p_c'}{p'} \cdot \frac{1}{n}\right)^{\frac{\lambda-\kappa}{\psi}} \cdot \left(\frac{p'}{p_i'}\right)^{\frac{\lambda}{\psi}} \cdot \frac{2(\eta - \alpha_0)}{M^2 - \eta_{K_{0nc}}^2} \quad (27)$$

where n = the yield stress ratio defined by the stress variable p'

$$n = \frac{\bar{p}_{c0}'}{p_i'} = \left(\frac{M^2 - \alpha_0^2 + (\eta_{K_{0nc}} - \alpha_0)^2}{M^2 - \alpha_0^2}\right) \cdot \frac{1 + 2K_{0nc}}{1 + 2K_0} \cdot \mathrm{OCR} \quad (28)$$

where $\mathrm{OCR} = \sigma_{p,24h}'/\sigma_{vi}'$ is the overconsolidation ratio measured from the 1D standard MSL_{24h} tests. If the soil is initially overconsolidated, the value of K_0 is generally larger than K_{0nc}.

At the end of undrained triaxial shearing tests, the critical state will be reached if the strains are large enough. Then the viscoplastic volumetric strain rate $\dot{\varepsilon}_v^{vp}$ becomes zero, and the stress ratio changes into M (compression) or $-M$ (extension). Under undrained condition, $\dot{\varepsilon}_s = \dot{\varepsilon}_a$, and when the soil sample is close to failure, it is reasonable to assume that $\dot{\varepsilon}_a \approx \dot{\varepsilon}_a^{vp}$. Therefore, by incorporating the expression of loading surface as Eq. (5) and the critical failure condition, the critical undrained shear strength ratio can be obtained from Eq. (27)

$$\left(\frac{S_{uc}}{\sigma_{vi}'}\right)_{c,e} = \frac{1 + 2K_0}{3} \cdot \frac{M}{2} \cdot \left(\frac{M \pm \alpha_0}{M} \cdot \frac{n}{2}\right)^\Lambda$$
$$\cdot \left(\frac{\dot{\varepsilon}_a}{\psi/(V_i T_0)} \cdot \frac{M^2 - \eta_{K_{0nc}}^2}{2(M \mp \alpha_0)}\right)^{\psi/\lambda} \quad (29)$$

where the subscripts c and e correspond to compressive and extensive conditions, respectively.

It can be seen that both the undrained compressive and extensive shear strengths depend on the axial strain rate. For two different strain rates $\dot{\varepsilon}_{a1}$ and $\dot{\varepsilon}_{a2}$, the strengths satisfy the relationship that

$$S_{u2}/S_{u1} = (\dot{\varepsilon}_{a2}/\dot{\varepsilon}_{a1})^{\psi/\lambda} \qquad (30)$$

Referring to Sheahan et al. (1996), a strain-rate parameter ρ can be defined to express the strain-rate dependency of the undrained shear strength

$$\rho = (\Delta S_u/S_{u1})/\Delta \log \dot{\varepsilon}_a \qquad (31)$$

where ΔS_u is the increment of S_u as the strain rate increases from $\dot{\varepsilon}_{a1}$ to $\dot{\varepsilon}_{a2}$. When a tenfold increase occurs in strain rates ($\dot{\varepsilon}_{a2} = 10\dot{\varepsilon}_{a1}$), ρ is a constant

$$\rho = 10^{\psi/\lambda} - 1 = 10^{C_\alpha/C_c} - 1 \qquad (32)$$

Comparison between Two Strain-Rate Parameters ρ_n and ρ

The strain-rate parameters ρ_n and ρ can describe the strain-rate dependencies of σ'_p and S_u, respectively. Their expressions are similar in form and both relate to the value of C_α/C_c. The value of ρ just depends on the ratio of $C_{\alpha R}/C_c$, but ρ_n relates to both C_α/C_c and Λ. Because Λ is smaller than the unit, ρ_n is always larger than ρ. Leroueil and Marques (1996) and Graham et al. (1983) indicated that the relationship between σ'_p and $\dot{\varepsilon}_z$ was almost a straight line whose slope was C_α/C_c in logarithmic scale. This conclusion is just an approximation because it ignores the elastic decrease of void ratio in the recompression phase [e.g., from point I to F in Fig. 3(a)]. In the presented model, the constant absolute time lines are used to simulate the viscous behavior of soils in 1D straining, and the differences of the elastic compressions before initial yielding under different strain rates are taken into account. Therefore, the obtained expression of ρ_n must be more accurate and feasible. Cheng and Yin (2005) also concluded that ρ_n are larger than ρ for natural Hong Kong marine clays.

For most inorganic clays, C_α/C_c equals to $0.03 \sim 0.05$ and Λ equals to $0.6 \sim 0.9$. Then, from Eq. (23) and Eq. (32), the value of ρ_n is obtained as $8\% \sim 21.2\%$, whereas ρ is in the range of $7.2\% \sim 12.2\%$. ρ_n is larger than ρ by $10\% \sim 80\%$ depending on the value of Λ. Table 1 and Table 2 summarize the measured values of ρ_n and ρ for different soils, respectively. It can be concluded that most measured results are in the predicted range. Additionally, the strain-rate parameter of strength ρ is independent of the consolidation history (isotropically or K_0-consolidated), consolidation stress, and test types (compression or extension). This feature of ρ is the same as most experimental results in the literature.

Actually, these two parameters ρ_n and ρ are just quantitatively defined to describe the strain-rate dependencies of preconsolidation

Table 1. Summary of Researches on Strain-Rate Dependency of Preconsolidation Pressures

Reference	Soil tested	ρ_n
Leroueil et al. (1985); Leroueil (1996)	Champlain clays (N)	$7 \sim 15\%$
Graham et al. (1983)	Ottawa clay (N)	16%
	Belfast clay (N)	20%
	Winnipeg clay (N)	10%
Nash et al. (1992)	Bothkennar clay (N)	$8 \sim 16.5\%$
Cheng and Yin (2005)	Aldrich Bay clay (N)	13.6%

Note: N. natural clays.

pressure and undrained strength, respectively. For some general loading paths (e.g., those with continuous changes of strain rates), the complete differential EVP model [i.e., Eq., (18)] must be used for prediction. As shown in the following, the soil behavior during creep, which is a typical process with continuous changes in strain rates, can be fairly well simulated by the proposed model.

Modeling the Strain-Rate Dependent Behavior of Soft Soils and Discussions

To verify the adequacy of the model, several triaxial undrained experimental results are predicted and compared with the literature.

Simulation of Undrained Triaxial Tests Sheared at Constant Strain Rate

Hinchberger and Rowe (2005) carried out undrained triaxial compression tests on Sackville clay. The soils were taken from the depth of $2 \sim 7$ m below a test embankment in the New Brunswick Province of Canada, and were normally consolidated to the stress $p'_i = 61.8$ kPa under the condition of $K_0 = 0.76$. The test strain rates were controlled to be 0.009%, 0.1%, and 1.14% per minute. Fig. 4 shows the experimental results of soil samples in the depth of 5.6 m. The soil parameters are given in Table 3, and M is backfigured to be 1.72. In addition, because the value of secondary compression coefficient C_α of Sackville clay is not given in the literature, ψ is assumed to be 0.035λ and 0.04λ in the present simulation. The predicted results are also shown in Fig. 4.

It can be noted that the calculated values of q increases faster than the measured results, especially in the early period of tests. The assumption of $C_\alpha/C_c = 0.035$ is relatively more suitable for Sackville clay, and the increasing rate of q becomes faster with larger value of ψ. However, generally, the predictions of the rate-dependent behavior of the anisotropically consolidated Sackville clay are considered to be good when the viscous parameter ψ is assumed to be 0.035λ.

Simulation of Undrained Triaxial Creep Tests

Hinchberger and Rowe (2005) also conducted some multistage undrained triaxial creep tests on normally consolidated Sackville clays. The applied deviator stresses q were 35, 44.5, and 50 kPa, respectively, and the soil sample was loaded to the next stage until the strains and excess pore pressure stabilized. Fig. 5 shows the comparison between the calculated and measured results. By using reasonable value of ψ $\psi = 0.035\lambda$, the theoretical increasing rate of axial strain is a little lower than the test results, but the general trend of axial strain during undrained creep has been described adequately. The simulated pore pressures increase faster with time than the measure results in the early test period, but they fit well with each other in the final stage, with the discrepancies in a narrow range of 10%.

The development of axial strain and pore pressure during undrained creep is closely related to the deviator stress q. When q is large enough, the axial strain rate will continuously increase, and this will accelerate the failure of soil. This creep failure does not happen on Sackville clay in the creep tests. Sekiguchi (1984) carried out similar creep tests on natural Osaka alluvial clay, which is distributed at Umeda. The undisturbed samples were firstly normally consolidated to the state of $p'_i = 294$ kPa, and then they were loaded with different values of q, which were in the range of $q/p'_i = 0.2 \sim 0.867$. The modeling parameters are given in Table 3. Most of the parameters are the same as those in that reference paper, except that κ is backcalculated by the given initial shear modulus G_0. Sekiguchi (1984) backfigured six creep rupture tests and

Table 2. Summary of Researches on Strain-Rate Dependency of Undrained Triaxial Shear Strengths

Reference	Soil tested	Test type	OCR	$\dot{\varepsilon}_a$(%/h)	ρ compression	ρ extension
Bjerrum et al. (1958)	Formebu clay (N)	CIUC	1.0	0.0036–10	13%	
Richardson and Whitman (1963)	Mississippi Valley alluvial clay (RS)	CIUC	1.0	0.12–60	3.5%	
Ladd et al. (1972)	Atchafalaya clay (N)	CIUC	1.0	0.5–60	10%	
Alberro and Santoyo (1973)	Mexico clay (N)	CIUC	1.0	0.045–94	9%	
Berre and Bjerrum (1973)	Drammen clay (N)	CAUC	1.0	0.0014–35	13%	
Vaid and Campanella (1977)	Haney clay (N)	CIUC	1.0	0.01–670	8%	
Hight (1983)	Lower clays (RS)	CAUC	1.0	0.04, 15	9%	
Graham et al. (1983)	Belfast clay (N)	CAUC	1.0	0.05–5.0	9.3%	
Graham et al. (1983)	Mastemyr clay (N)	CAUC, CAUE	1.0	0.003–0.4	9.4%	9.4%
Lefbvre and LeBoeuf (1987)	Various clays (N)	CI(A)UC	1.0	0.05–32	10%	
Kulhawy and Mayne (1990)	Marine clay	CIUC	1.0		10%	
Nakase and Kamei (1986)	Kawasaki clay	CIUC, CIUE	1.0		9.0%	9.0%
Cheng and Yin (2005)	HKMD (N)	CAUC, CAUE	1.0	0.2–20	8.5%	12.1%
Bjerrum et al. (1958)	Formebu clay (N)	CIUC	2.0	0.0036–10	10%	
Richardson and Whitman (1963)	Mississippi Valley alluvial clay (RS)	CIUC	16	0.12–60	6%	
Berre and Bjerrum (1973)	Drammen clay (N)	CAUC	1.5	0.0014–35	13%	
Hight (1983)	Lower clays (RS)	CAUC	4, 7	0.04–470	6%	
Sheahan et al. (1996)	Boston blue clay (RS)	CAUC	1 ~ 8	0.05–50	9.0%	
Zhu and Yin (2000)	HKMD (RS)	CIUC, CIUE	1 ~ 8	0.15–15	5.5%	8.4%

Note: CAUC/CAUE, anisotropic consolidated undrained triaxial test sheared in compression/extension; CIUC/CIUE, consolidated isotropic undrained triaxial test sheared in compression/tension; HKMD, Hong Kong marine deposits; N, natural clays; OCR = overconsolidation ratio; RS, reconstituted clays.
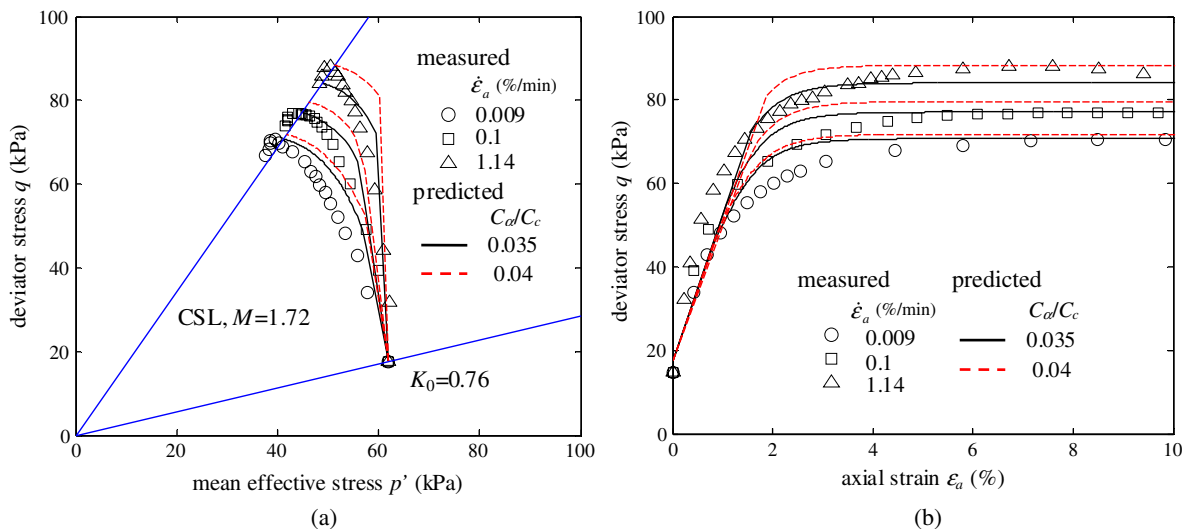
Zhu and Yin (2000)

Fig. 4. Predicted and measured results of undrained triaxial compression tests on Sackville clay; (a) the effective stress path; (b) the stress–strain relationship

Table 3. Values of the Modeling Parameters Used in the Prediction

Clay tested	κ/V_i	λ/V_i	ψ/V_i	M	$\varphi'_c(°)$	α_0	ν	OCR	Reference
Sackville clay	0.024	0.112	0.0039	1.72	42.0	0.586	0.3	1	Hinchberger and Rowe (2005)
Osaka clay	0.014	0.149	0.0059	1.26	31.3	0.601	0.3	1	Sekiguchi (1984)
Louiseville clay	0.033	0.225	0.009	1.32	32.8	0.582	0.3	2.2	Tanaka and Shiwakoti (2001)
Boston blue clay	0.022	0.164	0.0072	1.348	33.4	0.593	0.3	1–8	Sheahan et al. (1996)
HKMD	0.018	0.08	0.0032	1.265	31.5	0	0.3	1–8	Zhu and Yin (2000)

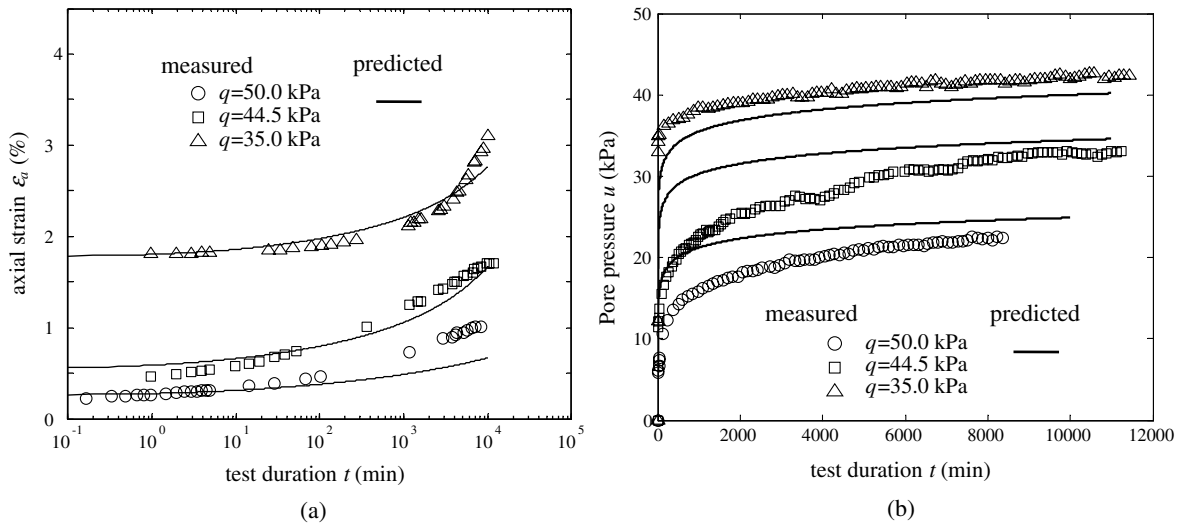Note: HKMD, Hong Kong marine deposits.

Zhu and Yin (2000)

Fig. 5. Predicted and measured results of undrained triaxial creep tests on Sackville clay; (a) axial strain versus test duration; (b) pore pressure versus test duration

obtained $M = 1.47$, which is much larger than that from other tests on the same Osaka alluvial clay reported in the literature. According to Adachi et al. (1985), the value of M should be 1.26. The predicted and measured results are shown in Fig. 6. It can be noted that when q/p_i' exceeds 0.663, the creep failure appears. The higher the value of q/p_i' becomes, the earlier the creep failure occurs. Although some discrepancies are observed, the general trend of creep failure and the corresponding rupture time can be fairly well described by this proposed model.

Investigation of the Rate Dependency of Preconsolidation Pressure

Fig. 7(a) shows the results of rate dependency of preconsolidation pressures for 12 natural marine clays from the Champlain sea area in Eastern Canada. The measured results with different markers are strictly from Leroueil and Tavenas (1983), and the preconsolidation pressures are normalized by the value from the CRS test whose

strain rate is $\dot{\varepsilon}_z = 4 \times 10^{-6} \text{s}^{-1}$. Because the features of these clays are similar, the modeling parameters of Louiseville clay (given in Table 3) are used to predict the relationship between σ_p' and $\dot{\varepsilon}_z$ for all these clays. The values of C_r and C_c are obtained from the compression curves of undisturbed Louiseville clay samples (Tanaka and Shiwakoti 2001), and then $\Lambda = 1 - C_r/C_c = 0.85$ C_α is assumed to be 0.04 C_c according to Leroueil and Marques (1996). It can be seen that the calculated results can adequately describe the relationships of σ_p' versus $\dot{\varepsilon}_z$, and most test data are in a narrow range of $\pm7\%$ from the predicted curve.

Fig. 7(b) shows the results of several natural marine clays from Finland. The test data and the soil markers are taken from Leroueil (1996). The values of the modeling parameters are assumed to be the same as those of Louiseville clay for their similar soil properties. Most of measured data equally distribute on the two sides of the calculated curve, and the increasing trend of σ_p' with the increase of $\dot{\varepsilon}_z$ is fairly assessed.
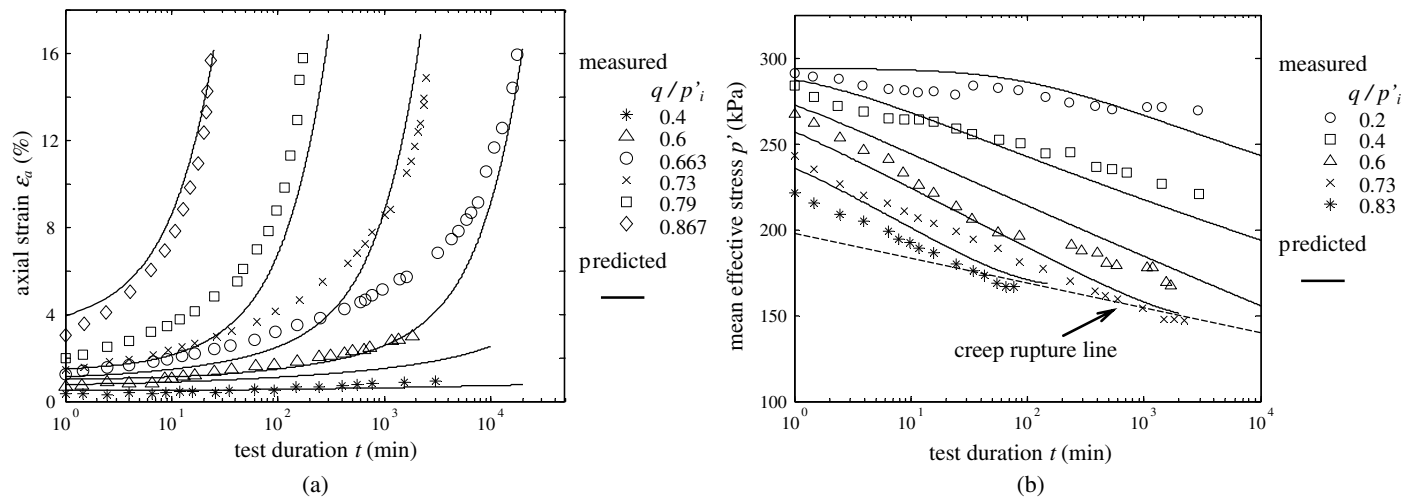

Fig. 6. Predicted and measured results of undrained triaxial creep tests on Osaka alluvial clay; (a) axial strain versus test duration; (b) mean effective stress versus test duration
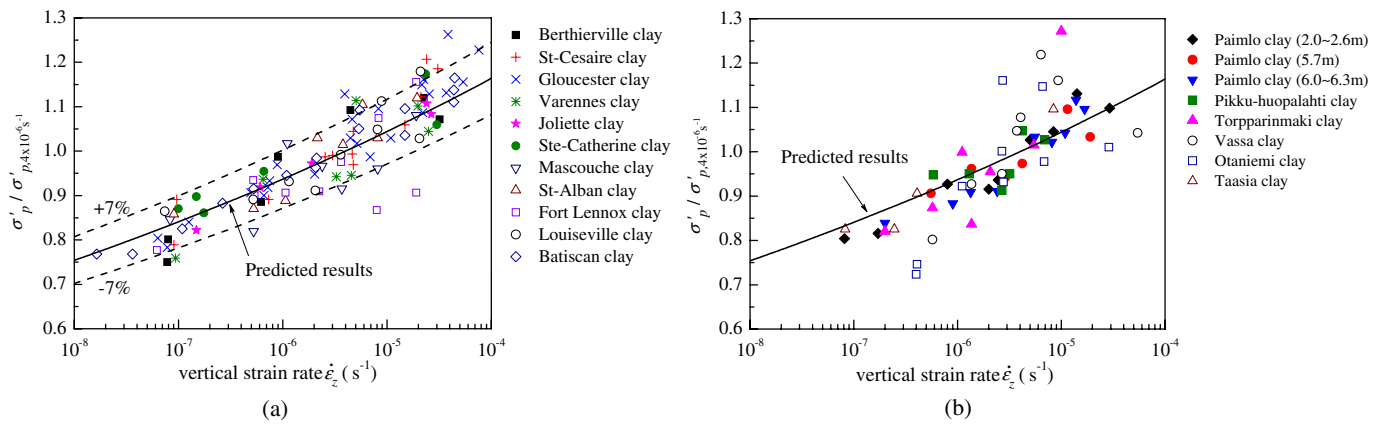
Fig. 7. Calculated and measured strain-rate dependency of preconsolidation pressure; (a) Champlain Sea clays; (b) Finnish clays

Table 4. Measured Values of $\sigma'_p/\sigma'_{p,24\,h}$ from Constant Rate of Strain Tests Whose Strain Rates Are $0.36 \sim 1.14\%$/h

Reference	Soil type	$\sigma'_p/\sigma'_{p,24\,h}$
Leroueil and Tavenas (1983)	Quebec, dozen of clays	1.28
Kolisoja et al. (1989)	Finland, one site	1.16
Hanzawa et al. (1990)	Osaka, Japan	$1.3 \sim 1.5$
Burghignoli et al. (1991)	Fucino, Italy	1.2
Hanzawa (1991)	Ariake Kuwana, Japan	$1.3 \sim 1.4$
Okumura and Suzuki (1990)	Yokohama, Japan	1.25
Hoikkala (1991)	Finland, three sites	1.3
Mizukami and Motoyashiki (1992)	Japan, several clays	1.18
Nash et al. (1992)	Bothkennar, U.K.	1.33
Cheng and Yin (2005)	Hong Kong, three sites	$1.14 \sim 1.36$

Fig. 8. Predicted and measured strain-rate dependency of compression strengths of K_0-consolidated Boston blue clay at different overconsolidation ratios

Table 4 gives the measured values of $\sigma'_p/\sigma'_{p,24\,h}$ for some other soils in the literature, and most of the testing strain rates are $0.36 \sim 1.44\%$/h. For most normally consolidated inorganic clays, the range of C_α/C_c is $0.03 \sim 0.05$, and Λ is $0.6 \sim 0.9$, then the calculated values of $\sigma'_p/\sigma'_{p,24\,h}$ from Eq. (20) are $1.08 \sim 1.36$. It can be seen that most measured results are within this predicted range. In general, the strain rate in the field is about $10^{-3}\%$/min, which is close to $\dot{\varepsilon}_{z,24\,h}$ (Leroueil and Tavenas 1983), so the value of $\sigma'_{p,24\,h}$ can be used directly for the in situ analysis. However, the values of σ'_p from other tests must be adjusted before applications for the strain-rate effects.

Simulation of the Strain-Rate Effects on Undrained Shear Strength

Fig. 8 and Fig. 9 show the effects of OCR on the strain-rate dependency of strengths. Fig. 8 illustrates the results of the reconstituted K_0-consolidated Boston Blue clays (BBCs), where the measured data are given by Sheahan et al. (1996). In the experimental procedures of BBC, for normally consolidated samples, a vertical consolidation stress of $\sigma'_{vi} = 290$ kPa was used, whereas the maximum vertical stress $\sigma'_v = 585$ kPa was maintained before unloading for overconsolidated samples. Fig. 9 shows the comparison between the predicted undrained strengths and measured data of Zhu and Yin (2000) for remolded isotropically consolidated Hong Kong marine deposits, and the preconsolidation pressure
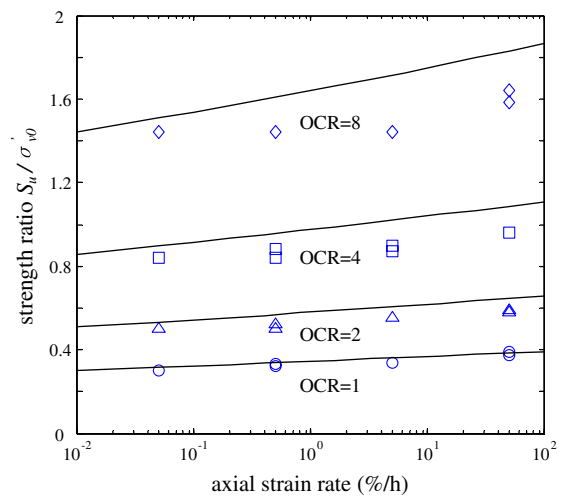
of each specimen is 392 kPa. The other modeling parameters of these two soils are shown in Table 3.

According to the results shown in Figs. 8 and 9, the predictions prove good. The trend that the strength ratios increase with strain rates is adequately described by this presented model, and the increasing rate of strength S_u versus axial strain rate $\dot{\varepsilon}_a$ becomes faster as OCR increases. It can also be found that the undrained strength S_u increases with OCR if the axial strain rate $\dot{\varepsilon}_a$ keeps constant. In general, the predicted curves are in accordance with the measured data, except that the soil samples are initially heavily overconsolidated (e.g., OCR = 8 in Fig. 8). This may be attributed to that the proportion of the elastic part in total compression becomes larger due to higher OCR, and the assumption $\dot{\varepsilon}_a \approx \dot{\varepsilon}_a^{vp}$ adopted in the theoretical prediction for undrained strength [as Eq. (29)] increases the errors accordingly. Although the proposed model can predict the strain-rate dependency of undrained strength behavior for overconsolidated clays, it is still not suggested to use this model in the condition with extreme high values of OCR (e.g., OCR > 8).
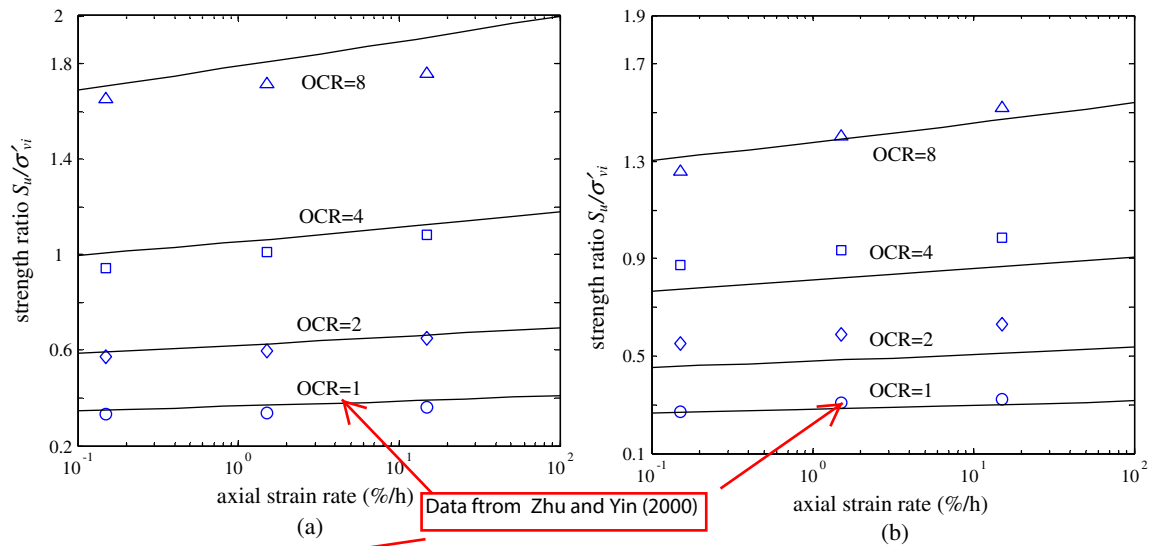
Fig. 9. Predicted and measured strain-rate dependency of strengths of Hong Kong marine deposits at different overconsolidation ratios; (a) compression tests (CIUC); (b) extension tests (CIUE)

All of the previous discussions demonstrate that the proposed EVP model has the capability of modeling the strain-rate dependent behavior of K_0-consolidated clays.

Conclusions

From this, the following conclusions can be obtained:

1. A new 3D anisotropic EVP constitutive model is presented to characterize the rate-dependent behavior of K_0-consolidated clays. Besides the loading surface f, a reference surface $\bar{f}$ corresponding to the reference time (i.e., $t_0 = 24$ h in this paper) is defined in the stress space. f can be either inside or outside of $\bar{f}$, and the viscoplastic strains would continue for all stress states except the stress origin.

2. With the application of absolute time t, the viscoplastic volumetric strain rate $\dot{\varepsilon}_{vn}^{vp}$ in the 1D straining can be expressed appropriately, and $\dot{\varepsilon}_{vn}^{vp}$ is just dependent on the difference between the current stress and its reference state, but independent of the $e - \ln \sigma_i'$ path.

3. The proposed model can adequately simulate the stress $\bar{f}$ strain behavior of undrained triaxial shear tests with constant strain rate of KR_0-consolidated clays. It can also fairly describe the trend of creep failure and the rupture life of undrained triaxial creep tests with high deviator stress.

4. The proposed theory can describe the strain-rate dependency of preconsolidation pressure, and the expression of corresponding strain-rate parameter ρ_n is given. In the CRS tests with strain rates of $0.36 \sim 1.14\%$/h and the parameters that $C_\alpha/C_c = 0.03 \sim 0.05$ and $\Lambda = 0.6 \sim 0.9$ for general inorganic clays, the calculated value of $\sigma_p'/\sigma_{p,24\,h}'$ is in the range of $1.08 \sim 1.36$, which agrees well with the literature.

5. The proposed theory can describe the strain-rate dependency of undrained triaxial shear strengths, and the expression of strain-rate parameter for strength ρ is given. The increasing rate of S_u with $\dot{\varepsilon}_a$ becomes faster as the value of OCR increases, and this feature can be fairly simulated by this model.

6. Different from ρ, ρ_n depends on not only the value of $C_\alpha R/C_c$ but also the compression parameter Λ, so ρ_n is generally larger than ρ. With the values of $C_\alpha R/C_c$ and Λ in

the above general range for inorganic clays, the calculated value of ρ_n is $8\% \sim 21.2\%$, whereas ρ is in the range of $7.2\% \sim 12.2\%$.

References

Adachi, T., and Oka, F. (1982). "Constitutive equations for normally consolidated clay based on elasto-viscoplasticity." *Soils Found.*, 22(4), 57–70.

Adachi, T., Mimura, M., and Oka, F. (1985). "Descriptive accuracy of several existing constitutive models for normally consolidated clays." *Proc., Fifth Int. Conf. Numerical Methods of Geomechanics*, Nagoya, Japan, 1, 259–266.

Alberro, J., and Santoyo, E. (1973). "Long term behaviour of Mexico city clay." *Proc., the 8th Int. Conf. on Soil Mechanics and Foundation Engineering*, Mockba, 1, 1–9.

Berre, T., and Bjerrum, L. (1973). "Shear strength of normally consolidated clays." *Proc., 8th Int. Conf. on Soil Mechanics and Foundation Engineering*, Mockba, 1, 39–49.

Bjerrum, L. (1967). "Engineering geology of Norwegian normally consolidated marine clays as related to the settlements of buildings." *Geotechnique*, 17(2), 83–118.

Bjerrum, L., Simons, N., and Toblaa, I. (1958). "The effect of time on the shear strength of a soft marine clay." *Proc., Conf. on Earth Pressure Problems*, 1, 148–158.

Burghignoli, A., et al. (1991). "Geotechnical characterization of Fucino clay." *Proc., 10th European Conf. on Soil Mechanics and Foundation Engineering*, 1, 329–378.

Cheng, C. M., and Yin, J. H. (2005). "Strain-rate dependent stress-strain behavior of undisturbed Hong Kong Marine deposits under oedometric and triaxial stress states." *Mar. Georesour. Geotechnol.*, 23(1–2), 61–92.

Desai, C. S., and Zhang, D. (1987). "Viscoplastic model for geologic materials with generalized flow rule." *Int. J. Numer. Anal. Methods Geomech.*, 11(6), 603–620.

Graham, J., Crooks, J. H. A., and Bell, A. L. (1983). "Time effects on the stress-strain behavior of natural soft clays." *Geotechnique*, 33(3), 327–340.

Hanzawa, H. (1991). "A new approach to determine the shear strength of soft clay." *Proc., Int. Conf. on Geotechnical Engineering for Coast Deviation, Geo-Coast-91*, 1, 23–28.

Hanzawa, H., Fuyaka, T., and Suzuki, K. (1990). "Evaluation of engineering properties for an Ariake clay." *Soils Found.*, 30(4), 11–24.

Hight, D. W. (1983). "Laboratory investigations of sea bed clays." Ph.D. thesis, Imperial College, Landon, U.K.

Hinchberger, S. D., and Rowe, R. K. (2005). "Evaluation of the predictive ability of two elastic-viscoplastic constitutive models." *Can. Geotech. J.*, 42(6), 1675–1694.

Hoikkala, S. (1991). "Continuous and incremental loading oedometer tests." M.S. thesis, Helsinki Univ. of Technology, Espoo, Finland.

Kelln, C., Sharma, J., Hughes, D., and Graham, J. (2008). "An improved elastic-viscoplastic soil model." *Can. Geotech. J.*, 45(10), 1356–1376.

Kolisoja, P., Sahi, K., and Hartikainen, J. (1989). "An automatic triaxial-oedometer device." *Proc., 12th Int. Conf. on Soil Mechanics and Foundation Engineering*, Rio de Janeiro, 1, 61–64.

Kulhawy, F. H., and Mayne, P. W. (1990). *Manual of estimating soil properties for foundation design*, Cornell Univ., Ithaca, NY.

Kutter, B. L., and Sathialingam, N. (1992). "Elastic-viscoplastic modeling of the rate-dependent behavior of clays." *Geotechnique*, 42(3), 427–441.

Ladd, C. C., Williams, C. E., Connell, D. H., and Edgers, L. (1972). "Engineering properties of soft foundation clays at two south Louisiana levee sites." *Research Report No. R72-26*, Massachusetts Institute of Technology, Cambridge, MA.

Lefebvre, G., and LeBoeuf, D. (1987). "Rate effects and cyclic loading of sensitive clays." *J. Geotech. Eng.*, 113(5), 476–489.

Leoni, M., Karstunen, M., and Vermeer, P. A. (2008). "Anisotropic creep model for soft soils." *Geotechnique*, 58(3), 215–226.

Leroueil, S. (1996). "Compressibility of clays: fundamental and practical aspects." *J. Geotech. Eng.*, 122(7), 534–543.

Leroueil, S., Kabbaj, M., Tavenas, F., and Bouchard, R. (1985). "Stress-strain-strain rate relation for the compressibility of sensitive natural clays." *Geotechnique*, 35(2), 159–180.

Leroueil, S., and Marques, M. E. S. (1996). "Importance of strain rate and temperature effects in geotechnical engineering." *Proc., Measuring and Modeling Time Dependent Soil Behavior*, T. C. Sheahan, and V. N. Kallakin, eds., ASCE, Reston, VA, 1–60.

Leroueil, S., and Tavenas, F. (1983). "Preconsolidation pressure of Champlain clays, Part II: laboratory determination." *Can. Geotech. J.*, 20(4), 803–816.

Li, X. S., and Dafalias, Y. F. (2004). "A constitutive framework for anisotropic sand including non-proportional loading." *Geotechnique*, 54(1), 41–55.

Liingaard, M., Augustesen, A., and Lade, P. V. (2004). "Characterization of models for time-dependent behavior of soils." *Int. J. Geomech.*, 4(3), 157–177.

Mesri, G., and Castro, A. (1987). "C_α/C_c concept and K_0 during secondary compression." *J. Geotech. Eng.*, 113(3), 230–247.

Mizukami, J. I., and Motoyashiki, M. (1992). "Consolidation yield stress by constant rate of strain test." *Proc., 28th Annual Conf. Japanese Society of Soil Mechanics and Foundation Engineering*, 419–420. (in Japanese).

Nakase, A., and Kamei, T. (1986). "Influence of strain rate on undrained shear characteristics of K_0 consolidated cohesive soils." *Soils Found.*, 26(1), 85–95.

Nash, D. F. T., Sills, G. C., and Davison, L. R. (1992). "One-dimensional consolidation testing of soft clay from Bothkennar." *Geotechnique*, 42(2), 241–256.

Okumura, T., and Suzuki, K. (1990). "Analysis of consolidation settlement considering the change in compressibility." *Proc., Int. Conf. on Geotechnical Engineering for Coast Deviation, Geo-Coast-91*, Yokohama, Japan, 1, 57–62.

Perzyna, P. (1963). "The constitutive equations for rate sensitive plastic materials." *Q. Appl. Math.*, 20(4), 321–332.

Richardson, A. M., and Whitman, R. V. (1963). "Effect of strain-rate upon undrained shear resistance of a saturated remoulded fat clay." *Geotechnique*, 13(4), 310–324.

Sekiguchi, H. (1984). "Theory of undrained creep rupture of normally consolidated clay based on elasto-viscoplasticity." *Soils Found.*, 24(1), 129–147.

Sheahan, T. C., Ladd, C. C., and Germaine, J. T. (1996). "Rate-dependent undrained shear behavior of a resedimented clay." *J. Geotech. Eng.*, 122(2), 99–108.

Tanaka, H., and Shiwakoti, D. R. (2001). "Comparison of mechanical behavior of two overconsolidated clays: Yamashita and Louiseville clays." *Soils Found.*, 41(4), 73–87.

Vaid, Y. P., and Campanella, R. G. (1977). "Time-dependent behavior of undisturbed clay." *J. Geotech. Engrg. Div.*, 103(7), 693–709.

Vermeer, P. A., and Neher, H. P. (2000). "A soft soil model that accounts for creep." *Proc., Int. Symposium on Beyond 2000 in Computational Geotechnics-10 Years of PLAXIS Int.*, Balkema, Rotterdam, 249–261.

Wang, L. Z., Shen, K. L., and Ye, S. H. (2008). "Undrained shear strength of K_0 consolidated soft soils." *Int. J. Geomech.*, 8(2), 105–113.

Wheeler, S. J., and Näätänen, A. (2003). "An anisotropic elastoplastic model for soft clays." *Can. Geotech. J.*, 40(2), 403–418.

Wood, D. M. (1990). *Soil behaviour and critical state soil mechanics*, Cambridge Univ. Press, U.K.

Yin, J. H., and Graham, J. (1994). "Equivalent times and one-dimensional elastic visco-plastic modeling of time-dependent behaviors of clays." *Can. Geotech. J.*, 31(1), 42–52.

Yin, J. H., and Graham, J. (1999). "Elastic viscoplastic modeling of the time-dependent stress-strain behaviour of soils." *Can. Geotech. J.*, 36(4), 736–745.

Zhou, C., Yin, J. H., Zhu, J. G., and Cheng, C. M. (2005). "Elastic anisotropic viscoplastic modeling of the strain-rate-dependent stress-strain behavior of KR_{0R}-consolidated natural marine clays in triaxial shear tests." *Int. J. Geomech.*, 5(3), 218–232.

Zhu, J. G., and Yin, J. H. (2000). "Strain-rate dependent stress-strain behaviour of overconsolidated Hong Kong marine clay." *Can. Geotech. J.*, 37(6), 1272–1282.